sciendo

Journal of Horticultural Research 2022, vol. 30(2): 23–32
DOI: 10.2478/johr-2022-0013

© The Author(s) 2022. This article is distributed under the terms of the Creative Commons Attribution 4.0 International License (http://creativecommons.org/licenses/by/4.0/).

MODELING AND ANALYSIS OF ROOT BRANCHING PLASTICITY BASED ON PARRONDO'S GAME

Songyang LI*, Miao WANG, Haipeng YU
Henan University of Engineering, China

Received: December 2021; Accepted: July 2022

ABSTRACT

For different kinds of plants, the distribution of lateral roots is highly plastic in different growth environments. In particular, the branching distance of the roots plays a decisive role in the formation of the root system architecture. In many root-system architecture models, constant branching distances of different branching orders usually are used to simulate the dynamics of a root system architecture. However, little is known about the formation of lateral roots, and branching distances for different branching orders are variable in the actual root system. The resource allocation model for predicting the lateral root distribution in individual plants has been established based on Parrondo's game. The root branching data predicted by the model is compared with the actual root branching data. The results show that the proposed method can cause serious changes in the spacing and distribution of lateral root formation. A parameter called development window can be used to override interbranch distance in the root-system architecture models.

Key words: Parrondo's game, root system architecture, branching density, interbranch distance, resource allocation model

INTRODUCTION

The plant's root system is an essential part of the plant's body. It not only anchors the plant in its substrate, extracts water and minerals, and transports them from the ground, but also is a synthesis site for many metabolites (Dubrovsky et al. 2006). Root elongation and branching are the most important ways of plant adaptation in the modulation of the architecture of the root system to ensure adequate resources (nitrogen, water, etc.) (Ötvös et al. 2021). For example, the growth and development of lateral roots can be regulated by different temporal or spatial distribution of nutrients. The emergence of lateral roots in Arabidopsis can be inhibited with a homogeneous high nitrate level and promoted with a homogeneous low nitrate level (Gifford et al. 2008). When Arabidopsis grows at homogeneous low nitrate levels, the emergence of lateral roots may increase when transferred to heterogeneous high nitrate levels (Zhang & Forde 1998). When Arabidopsis grows under dynamic nitrate distribution, more lateral roots develop in the high nitrate zone to explore the soil (Giehl et al. 2012). In the split-root pea experiment, more lateral roots are found in the high nitrate region than in the low nitrate region (Dener et al. 2016). The results show that lateral root primordia can perceive the surrounding soil environment and communicate with other lateral root primordia (McCleery et al. 2017; Cabal et al. 2020).

The plasticity of lateral roots leads to a very complex root system architecture. In addition, the root system is buried in an opaque medium. It is difficult to observe and quantify it directly. Root architecture models are excellent tools for recreating actual root architectures and identifying root plasticity, so they can be used for plastic analysis

*Corresponding author
e-mail: asonglg@qq.com

or environmental stimulus evaluation (Muller et al. 2019). The ROOTMAP model defines lateral root formation using branching density and duration of apical nonbranching. The time of appearance of each branching order is given by the sum of the time of appearance of the previous branching order, the duration of apical nonbranching for the previous branching order, and the growth time required by the previous order (Diggle 1988). Then, models of root system architecture (RootTyp, ArchiSimple, CRootBox, OpenSimRoot, DigR, etc.) are proposed for modeling and simulating root growth and development (Barczi et al. 2018). These models usually use parameters such as interbranch distance (IbD), interprimordium distance, or branching frequency to describe lateral root formation. The above models can reproduce complex and varied lateral root growth patterns according to parameters such as IbD, which depends on environmental conditions near the root tip. However, due to the lack of branching data on the diversity of root responses to the soil environment, IbD in the above models cannot be estimated from actual root growth data. Additional studies are required to simulate the variation of the IbD in the roots and their plasticity under local conditions (Pagès 2019).

In order to model and simulate the observed root branching changes, Parrondo's game-based resource allocation model is proposed to predict the effects of competition and collaboration between lateral root primordia on lateral root emergence. According to the rhizomer hypothesis, the roots can be viewed as a swarm of coupled rhizomers. The rhizomer can sense the local environment and interact with adjacent rhizomers through both short- and long-range signals. The emergence of lateral roots is the result of decision-making by the swarms of the rhizomers (McCleery et al. 2017). Parrondo's game is then used to model short- and long-range signal transmission and redistribute all resources between rhizomers. The model can allow for a better understanding the clue signals that operate successively throughout the branching process. Finally, the proposed method is simulated and verified on the basis of eight different plant root samples (six species) observed in homogeneous soils (Pagès 2019).

MATERIALS AND METHODS

Resource allocation model based on Parrondo's game

According to the rhizomer hypothesis, rhizomers can be defined as a repeating development window along the mother root axis, centered around a primed prebranch site that is able to develop into a lateral root. Prebranch sites are established after a period of oscillation in the zone between the root basal meristem and the elongation zone. Within a narrow development window, a primed prebranch site may initiate the formation of a lateral root primordium (McCleery et al. 2017). In this article, we assume that the initiation of the primordium naturally follows priming and always occurs acropetally. Therefore, a swarm of rhizomers can be obtained from the approximate length of the rhizomers calculated by the oscillating gene expression (Fig. 1). Each rhizomer contains a primed prebranch site where a single lateral root can develop. The rhizomer can sense the local environment and interact with adjacent rhizomers to make root branching decisions to achieve an adaptive response.

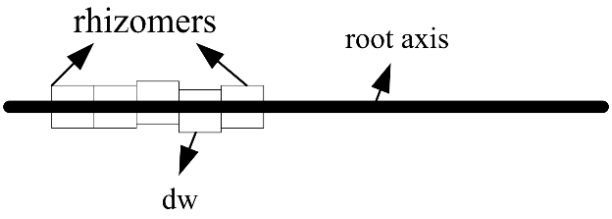


Figure 1. Schema of rhizomers based on development window (dw)

According to McCleery et al. (2017), there are short- and long-range signal pathways among rhizomers. Short-range signal pathways allow rhizomers to interact with their immediate neighbors and soil conditions. For example, AUX1 reacts with iron, and TIR1 responds to phosphate. Local stimuli may also favor auxin accumulation. The dual-transceptor NRT1.1 perceives nitrates and transports auxin, translating local high nitrate soil conditions into auxin accumulation.

Long-range signal pathways pass through the phloem and xylem, as well as through the path of auxin polar transport for communication between nonadjacent rhizomers. For example, in split-root

experiments, each root is in a different soil environment. The output signal from the roots must be conveyed to the entire root system.

The rhizomer hypothesis assumes that adjacent rhizomers may participate in short-range signal transmission through cell-to-cell transport and apoplastic diffusion. Rhizomers also communicate with all other rhizomers through a long-range signal through diffusion and vascular flow.

Thus, the roots can be viewed as a set of rhizomers. Inspired by Parrondo's game, the resource allocation model is established among the rhizomers. Parrondo's game says that there are two losing gambling games. When two games alternate periodically or randomly (AABB, ABAB, etc.), they become the winning result (Harmer & Abbott 1999). Since the fate of lateral root primordium is not unique, it means that the primordium may or may not emerge (Muller et al. 2019). There is cooperation and competition between the rhizomers.

Parrondo's Game A is constructed to model short-range signals between adjacent rhizomers. It is used to model competitive the relationship between adjacent rhizomers. Each rhizomer should maximize its own resource acquisition to achieve its own emergence.

Parrondo's Game B is constructed to model long-range signals among all rhizomers. That means that all rhizomers should emerge to maximize resource costs. Thus, rhizomers with fewer resources are more likely to gain resources from long-range signals, while rhizomers with more resources are less likely to gain resources from long-range signals. Game B is used to model the cooperative relationship between the rhizomers. This strategy represents the potential goal of optimizing the root system. The model of resource allocation among rhizomers is shown in Figure 2.

Game A is used to model the competition between adjacent rhizomers. Each rhizomer should maximize its own resource acquisition to achieve its own emergence. Adjacent rhizomers can compete for resources through cell-to-cell transport and apoplastic diffusion. This means that one rhizomer will increase resources, while the adjacent rhizomer will reduce resources. In the model, we use zero-sum Parrondo's Game A to model the process.

Game B is a negative-sum game used to model cooperative relations between rhizomers. There is a cooperative relationship between the rhizomers. This means that all rhizomers should emerge to maximize resource costs. Therefore, a rhizomer with fewer resources has a higher probability (p1) of obtaining resources, while a rhizomer with more resources has a lower probability (p2) of obtaining resources. This strategy represents a potential of root system optimization target (Ye et al. 2013).

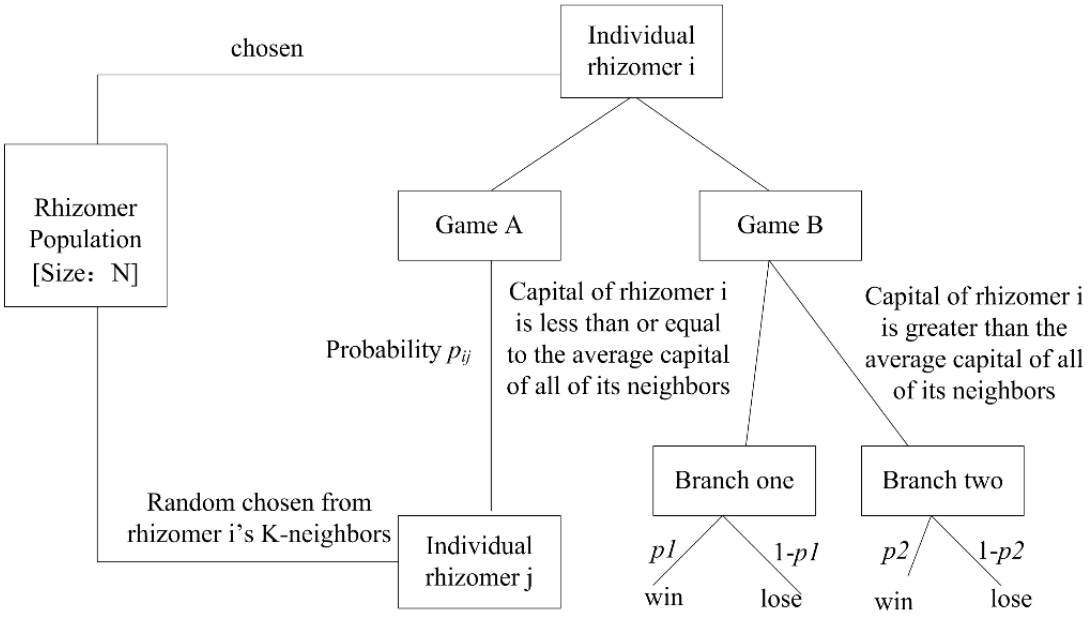


Figure 2. Structure of Parrondo's game of rhizomers

The resource allocation between rhizomers is described as follows.

(1) Single root divided into N rhizomers by given development window.

(2) Choose the i_{th} rhizomer.

(3) Get K-nearest neighbor (KNN_i) of i_{th} rhizomer and choose individual j_{th} rhizomer from KNN_i; the K-nearest neighbor (KNN_i) of the i_{th} rhizomer can be defined as the set of rhizomers i-K/2 to i+K/2. K is an even number.

(4) Play the zero-sum Game A between rhizomer i and j. Game A can change the capital redistribution of rhizomer i and j; the winning probability of the rhizomer i to the rhizomer j is p_{ij} (Equation 1). If rhizomer i wins, it will increase capital by one unit, and rhizomer j will decrease capital by one unit. If rhizomer i loses, it will reduce capital by one unit, and rhizomer j will increase capital by one unit:

$$p_{ij}(t) = \frac{W_i(t)}{W_i(t) + W_j(t)} \quad (1);$$

where $W_i(t)$ is the cumulative capital of the rhizomer i at time t, and $W_j(t)$ is the cumulative capital of the rhizomer j at time t.

(5) Play a negative-sum Game B. Game B can change the capital distributions between all rhizomers; Game B has two branches (branch 1 and branch 2); when the capital of rhizomer i is less than or equal to the average capital of the KNN neighbors, branch 1 will be done; the probability of winning the rhizomer i is p1 (Equation 2); when the capital of rhizomer i is greater than the average capital of the KNN neighbors, branch 2 will be done; the probability of winning the rhizomer i is p2 (Equation 3); if the rhizomer i wins, it will increase the capital by one unit; otherwise, it will reduce the capital by one unit:

$$p1 = p1_0 - \varepsilon * E_i \quad (2);$$

$$p2 = p2_0 - \varepsilon * E_i \quad (3);$$

where parameters $p1_0$ and $p2_0$ are the maximum winning probabilities of p1 and p2; and ε is the biases. Probability p1 is greater than p2. Branch 1 of Game B is the favorable branch. This means that rhizomers with fewer resources are more likely to gain resources. These parameters are not chosen arbitrarily. According to Harmer and Abbott (1999), we should set the correct p1 and p2 values (such as p1 = 0.75, p2 = 0.1) to ensure that Game B is a losing game; E_i is the local environment factor sensed by the rhizomer i, and can be calculated using Equation 4:

$$E_i = 1 - \min\left\{ \frac{E_{i_upt} - E_{i_\min}}{E_{i_opt1} - E_{i_\min}} > 0,\quad 1,\quad \frac{E_{i_upt} - E_{i_opt2}}{E_{i_\max} - E_{i_opt2}} > 0 \right\} \quad (4);$$

where E_{i_min} is the minimum resource demand; E_{i_opt1} is the lower limit of the optimal resource demand; E_{i_opt2} is the upper limit for the optimal resource demand; E_{i_max} is the maximum resource demand; and E_{i_upt} is the number of resources (Li et al. 2016).

(6) Repeat steps 2 through 5 to traverse the entire rhizomer; if the capital of the rhizomer i reaches the given threshold (R_{thr}) and the age of the rhizomer i is in the given growth cycle ($RAge_{max}$), it will emerge on a branch. If the rhizomer i capital does not reach the given threshold (R_{thr}) in the given growth cycle ($RAge_{max}$), it will continue to develop; otherwise, the rhizomer i will be dormant unless a new stimulus arises.

Model evaluation process

In order to evaluate the proposed model, a simple and generic root model (ArchiSimple) is used to control root growth (Pagès et al. 2014). The root elongation is calculated by Equation 5.

$$\begin{aligned} &PER = EL * D \quad D > D_{\min} \; and \quad Age < GD \\ &PER = 0 \quad D \le D_{\min} \; or \quad Age \ge GD \\ &GD = GD_s * D^2 \end{aligned} \quad (5);$$

where PER is the potential elongation rate; EL is the slope of the potential elongation rate versus diameter ($mm \cdot mm^{-1} \cdot day^{-1}$); GD is the duration of root growth (day); D_{min} is the minimum threshold diameter below which there is no possible elongation (mm); D is the apical diameter (mm); Age defines the root age (day); and GD_s is the growth duration parameter ($day \cdot mm^{-2}$).

As we know, the IbD must be greater than the development window. According to the published paper (Pagès 2019), the IbD is from 0.4 to 4.6 mm. In this article, we assume that the development window of each plant sample is between 0.4 mm and IbD. For each sample of each species, the development window value is in the set DW = {0.4, 0.4 + Δd, 0.4 + 2*Δd, … ,0.4 + i*Δd, IbD}. Δd is the spacing that is set 0.05 mm. The tip diameters of each sample of each species are stored in the set D_i (Equation 6).

$D_i = \{d_{ij}\}\ i \in \{$AnOdPC, AnOdN, ArElPC, DaGlN, LoPeT, PoTrPC, PoTrT, ZeMaPC$\}$ (6);

where d_{ij} is the value of the j_{th} tip diameter of the i_{th} sample; AnOdPC, AnOdN, ArElPC, DaGlN, LoPeT, PoTrPC, PoTrT, and ZeMaPC are the abbreviations of the plant sample shown in Table 1.

We use a simple iterative method to predict lateral root branching and verify the proposed model. For each sampled root (d_{ij}), we calculate the root branching mode by repeatedly selecting different development window values according to Equation 4 and the resource allocation model. We then calculate the predicted branching probability density (PBRD) under development window and compare PBRD with the actual branching probability density of the i_{th} sample data. We will use AnOdPC as an example to illustrate the evaluation process.

Step 1. Pick development window from DW.

Step 2. When Age of AnOdPC is less than GD, the root elongation is calculated from Equation 5. The resource between the rhizomers are allocated based on Parrondo's game. When Age of AnOdPC is greater than or equal to GD, the root stops elongation. Predicted root branching data can be obtained.

Step 3. Repeat steps 1 and 2. Finally, compare the predicted root branching data (called predicted) and the actual root branching data (called empirical) of AnOdPC.

RESULTS

Parameters values and dataset

The evaluation is made using various data sources from published papers (Table 1). The parameters of Parrondo's game are shown in Table 2. In the following, we will illustrate the procedure for six different species and eight different samples (*Anthoxanthum odoratum*, *Arrhenatherum elatius*, *Dactylis glomerata*, *Lolium perenne*, *Poa trivialis*, and *Zea mays*). The growth environment, excavation, and root system measurements are described in the published papers by Pagès and Picon-Cochard (2014) and Pagès (2019).

Table 1. List of considered samples, with the name of the species, the family, the site of observation, the abbreviation, and parameters values for elongation of each species

Species	Family	Site	Sample abbreviation	EL	GDs	D_{min}	IbD
Anthoxanthum odoratum	Poaceae	Pot Clermont-Ferrand	AnOdPC	18.8(2.4)	774	0.07	1.43(0.072)
Anthoxanthum odoratum	Poaceae	Nozeyrolles	AnOdN	18.8(2.4)	774	0.07	1.43(0.072)
Arrhenatherum elatius	Poaceae	Pot Clermont-Ferrand	ArElPC	17.6(1.2)	302	0.098	3.78(0.070)
Dactylis glomerata	Poaceae	Nozeyrolles	DaGlN	14.7(1.3)	803	0.075	2.43(0.071)
Lolium perenne	Poaceae	Thouzon	LoPeT	16.6(1.7)	1533	0.058	2.44(0.069)
Poa trivialis	Poaceae	Pot Clermont-Ferrand	PoTrPC	25.8(1.1)	1407	0.051	1.09(0.067)
Poa trivialis	Poaceae	Thouzon	PoTrT	25.8(1.1)	1407	0.051	1.09(0.067)
Zea mays	Poaceae	Pot Avignon	ZeMaPC	51	50	0.14	2

Table 2. Parameters for Parrondo's game

Name	Description	Unit	Value
$p1_0$	maximum winning probability of branch 1	-	0.75
$P2_0$	maximum winning probability of branch 2	-	0.1
R_{thr}	capital threshold of rhizomer	-	5
$RAge_{max}$	growth duration of rhizomer	day	5
K	K-nearest neighbor	-	2
ε	biases	-	0.005
EL	slope of potential elongation rate versus diameter	$mm \cdot mm^{-1} \cdot day^{-1}$	according to species
GDs	growth duration parameter	$day \cdot mm^{-2}$	according to species
D_{min}	minimum threshold diameter below which there is no possible elongation	mm	according to species

Evaluation of resource allocation model

The experiments were carried out on the Windows 10 operating system and Intel(R) Core(TM) i7-10700 CPU 2.90 GHz, 16 GB memory, Matlab R2021a simulation software. According to the evaluation process mentioned, predicted branching data can be collected. Then an estimate of the kernel smoothing function (ksdensity function of Matlab R2021a) is used to estimate the probability density of the simulated prediction and actual sample data. The mean-squared error (immse function of Matlab R2021a) is used to evaluate the quality of the fit between simulated prediction and actual sample data.

We use different development window values of each sample to calculate the mean-squared errors between the simulated prediction and the actual sample data to evaluate the quality of the fit. Figure 3 shows the probability density distributions of eight samples according to the minimum mean-squared error.

The results show that the two best matches were obtained for AnOdPC and ArElPC (Fig. 3). The other simulated distributions are also very close to the actual distributions. The overall shape and skewness are also well rendered. Most of them, with the exception of PoTrPC, slightly underestimated the probability density.

Figure 4 shows the shape of the mean-squared errors between the simulated distributions and the actual IbD distributions. In the case of AnOdN, AnOdPC, PoTrPC, ZeMaPC, DaGlN, and LoPeT species, they have similar mean-squared error change processes. When the development window value changes from low to high, the mean-squared error between the simulated distributions and the actual IbD distributions first decreases and then increases. This phenomenon is particularly evident in the case of DaGlN and LoPeT.

A very interesting phenomenon is that the mean-squared errors of ArElPC, PoTrT, and LoPeT have oscillation characteristics. This phenomenon is particularly evident in ArElPC and PoTrT. There are many development window values that can cause a small mean-squared error.

Within species, the mean-squared error shapes also vary. For AnOdN and AnOdPC, the optimal development window values range from 1.05 mm to 1.25 mm, and the error curves are similar. In the case of PoTrT and PoTrPC species, the error curves differ significantly.

Parameter sensitivity analysis

In the resource allocation model, setting the probability $p1_0$ and $p2_0$ has a significant effect on predicting root branching. Figure 5 shows the mean-squared error curves of DaGlN (Fig. 5A) and AnOdPC (Fig. 5B), which are influenced by different settings of $p1_0$ and $p2_0$. In the upper parts of Figures 5A, B, the $p1_0$ values remain unchanged. The $p2_0$ values are set to 0.15, 0.1, and 0.05, respectively. In the lower parts of Figures 5A, B, the $p2_0$ values remain unchanged. The $p1_0$ values are set to 0.8, 0.75, and 0.7, respectively. The optimal values for the development window are also around 1 mm. The results show that although the change of parameters has an impact on the mean-squared error, it has a limited impact on obtaining the optimal development window.

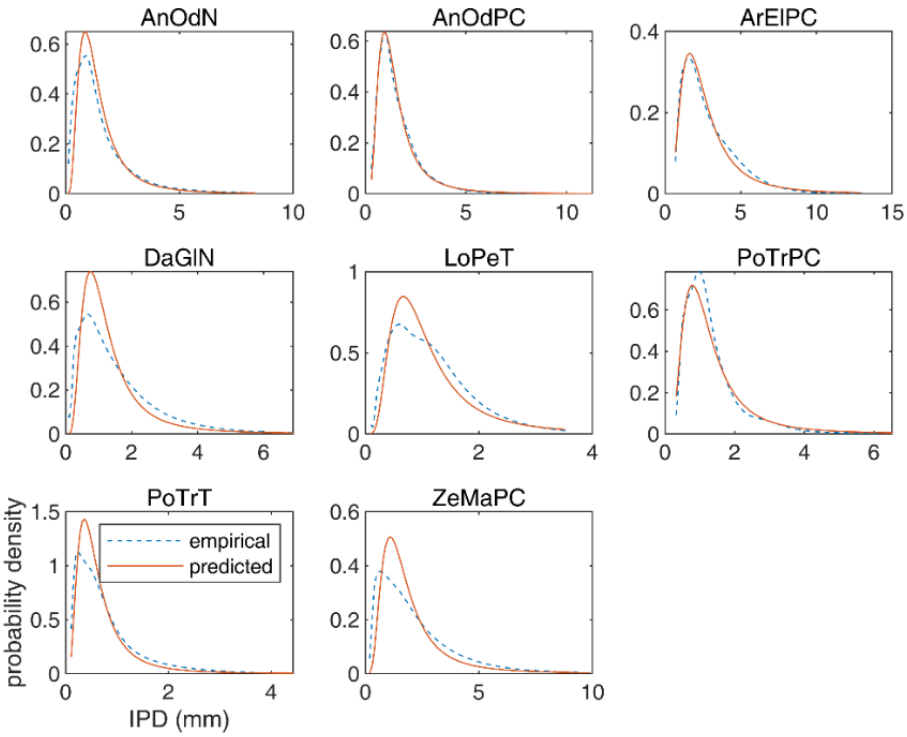


Figure 3. Probability density distributions of eight samples to illustrate best fit of the model according to the mean-squared error. Solid lines are simulated distributions, and dashed lines are observed distributions

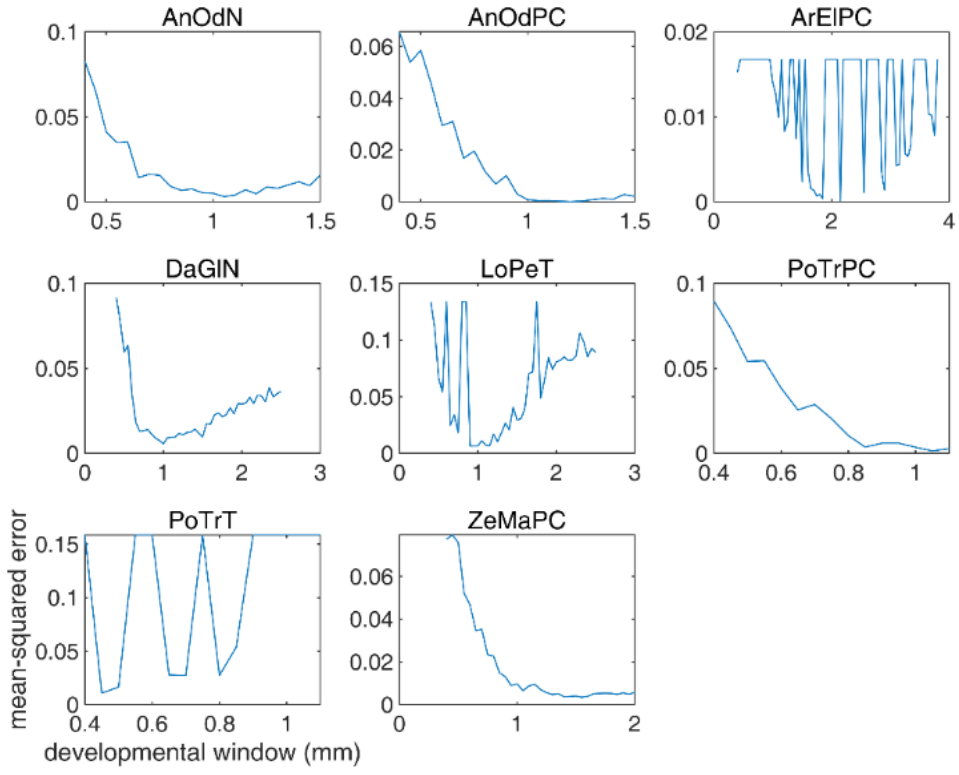


Figure 4. Mean-squared errors of eight samples between simulated distributions and the empirical IbD distributions

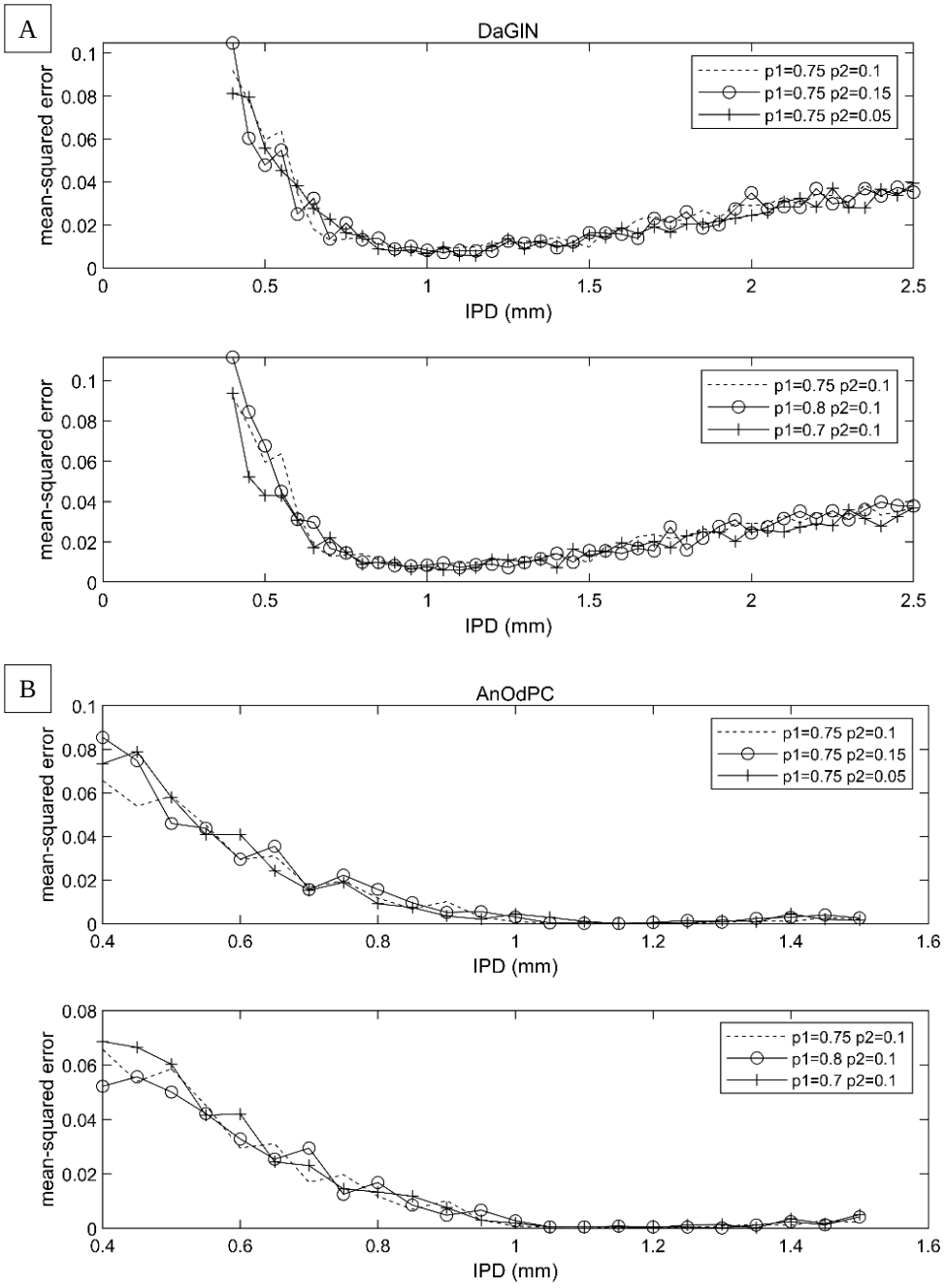


Figure 5. Mean-squared errors of DaGlN (A) and AnOdPC (B) with different p1 and p2

DISCUSSION AND CONCLUSIONS

According to Parrondo's game, the branching pattern of the roots can be predicted and evaluated based on a dataset of eight samples from six species. As we know, the spacing and distribution of lateral roots are critical determinants of the architecture of the plant root system. Auxin, cytokinin, or other hormones directly or indirectly affect cell fate in different ways in lateral root formation. Auxin biosynthesis, polar transport, and signal transduction are key processes in promoting lateral root development (Jing & Strader 2019). The proposed model uses rhizomer capital to determine the emergence of lateral roots. We can easily associate capital with auxin or cytokinin to simulate hormone redistribution to investigate the underlying mechanisms of lateral root formation.

This model can be integrated with root-system architecture models such as ArchiSimple as a component (Pagès et al. 2014). In root-system architecture models, the branching density or constant IbD is usually used to model the branching process of the root system. However, several models of the root system architecture can generate near-real root systems. This means that the IbDs of the above models are constant values. The IbD is highly plastic depending on the species. Even for the same species, the IbD varies considerably. Based on Figures 3 and 4, we can find a suitable and relatively stable development window value for each sample to obtain different branching distances. Thus, we are in line with Pagès's view (Pagès 2019), and we also suggest using the development window to model branch spacing diversity.

The results in Figure 4 show some interesting phenomena. Some mean-squared error curves are oscillating, and some mean-squared error curves are nonoscillating. Even for the same species, the PoTrT curve is oscillatory, but PoTrPC is not oscillatory. The diameter distribution of the PoTrPC tip is relatively concentrated in a smaller range than that of PoTrT. The development window value can be influenced by the thick- or fine-tip diameter for PoTrT and ArElPC samples. However, for other samples (AnOdN, AnOdPC, PoTrPC, ZeMaPC, DaGlN, and LoPeT), the development window values are not affected by the root diameter.

The results show that the development window can better describe the plasticity of the lateral root branching. It avoids the root branching deficiency in popular models of root architecture. The proposed method may support virtual plant research and promote the use of root modeling and simulation in precision agriculture.

Acknowledgments

This work was supported by the National Natural Science Foundation of China (61501174, U1704124), the Key Scientific Research Projects of Henan Province (21A520005, 20A520010), and the Scientific and Cultivation Fund of Henan University of Engineering (PYXM202020).

REFERENCES

Barczi J.F., Rey H., Griffon S., Jourdan C. 2018. DigR: a generic model and its open source simulation software to mimic three-dimensional root-system architecture diversity. Annals of Botany 121(5): 1089–1104. DOI: 10.1093/aob/mcy018.

Cabal C., Martínez-García R., de Castro Aguilar A., Valladares F., Pacala S.W. 2020. The exploitative segregation of plant roots. Science 370(6521): 1197–1199. DOI: 10.1126/science.aba9877.

Diggle A.J. 1988. ROOTMAP – a model in three-dimensional coordinates of the growth and structure of fibrous root systems. Plant and Soil 105(2): 169–178. DOI: 10.1007/bf02376780.

Dener E., Kacelnik A., Shemesh H. 2016. Pea plants show risk sensitivity. Current Biology 26(13): 1763–1767. DOI: 10.1016/j.cub.2016.05.008.

Dubrovsky J.G., Gambetta G.A., Hernández-Barrera A., Shishkova S., González I. 2006. Lateral root initiation in *Arabidopsis*: developmental window, spatial patterning, density and predictability. Annals of Botany 97(5): 903–915. DOI: 10.1093/aob/mcj604.

Giehl R.F.H., Lima J.E., von Wirén N. 2012. Localized iron supply triggers lateral root elongation in *Arabidopsis* by altering the AUX1-mediated auxin distribution. Plant Cell 24(1): 33–49. DOI: 10.1105/tpc.111.092973.

Gifford M.L., Dean A., Gutierrez R.A., Coruzzi G.M., Birnbaum K.D. 2008. Cell-specific nitrogen responses mediate developmental plasticity. Proceedings of the National Academy of Sciences 105(2): 803–808. DOI: 10.1073/pnas.0709559105.

Harmer G.P., Abbott D. 1999. Losing strategies can win by Parrondo's paradox. Nature 402(6764): 864. DOI: 10.1038/47220.

Jing H., Strader L.C. 2019. Interplay of auxin and cytokinin in lateral root development. International Journal of Molecular Sciences 20(3); 486; 12 p. DOI: 10.3390/ijms20030486.

Li S., Liu X., Wang M., Yu W. 2016. Exploring root plasticity to resource patches based on swarm behavior. Acta Physiologiae Plantarum 38(8); 192; 10 p. DOI: 10.1007/s11738-016-2227-2.

McCleery W.T., Mohd-Radzman N.A., Grieneisen V.A. 2017. Root branching plasticity: collective decision-making results from local and global signalling. Current Opinion in Cell Biology 44: 51–58. DOI: 10.1016/j.ceb.2017.03.001.

Muller B., Guédon Y., Passot S., Lobet G., Nacry P., Pagès L. et al. 2019. Lateral roots: Random diversity in adversity. Trends in Plant Science 24(9): 810–825. DOI: 10.1016/j.tplants.2019.05.011.

Ötvös K., Marconi M., Vega A., O' Brien J., Johnson A., Abualia R. et al. 2020 Modulation of plant root growth by nitrogen source-defined regulation of polar auxin transport. EMBO Journal 40(3); 106862; 21 p. DOI: 10.15252/embj.2020106862.

Pagès L. 2019. Analysis and modeling of the variations of root branching density within individual plants and among species. Frontiers in Plant Science 10; 1020; 10 p. DOI: 10.3389/fpls.2019.01020.

Pagès L., Picon-Cochard C. 2014. Modelling the root system architecture of Poaceae. Can we simulate integrated traits from morphological parameters of growth and branching? New Phytologist 204: 149–158. DOI: 10.1111/nph.12904.

Pagès L., Bécel C., Boukcim H., Moreau D., Nguyen C., Voisin A.-S. 2014. Calibration and evaluation of ArchiSimple, a simple model of root system architecture. Ecological Modelling 290: 76–84. DOI: 10.1016/j.ecolmodel.2013.11.014.

Ye Y., Wang L., Xie N. 2013. Parrondo's games based on complex networks and the paradoxical effect. PLoS One 8(7); e67924; 11 p. DOI: 10.1371/journal.pone.0067924.

Zhang H., Forde B.G. 1998. An *arabidopsis* MADS box gene that controls nutrient-induced changes in root architecture. Science 279(5349): 407–409. DOI: 10.1126/science.279.5349.407.